# $\label{eq:hicum/L0} HICUM\,/\,L0$ A simple compact heterojunction bipolar transistor model

Technical documentation of model version 2.0.0

Author:

M. Schroter

Copyright © Michael Schroter 2001-2019

This work is licensed under the Creative Commons Attribution 4.0 International License. To view a copy of this license, visit http://creativecommons.org/licenses/by/4.0/ or send a letter to Creative Commons, PO Box 1866, Mountain View, CA 94042, USA.

# List of often used symbols and abbreviations

 $A_{E0}$  ,  $L_{E0}$   $\;\;$  emitter window area and perimeter

A<sub>E</sub> , L<sub>E</sub> effective (electrical) emitter area and perimeter

 $b_{E0}$ ,  $l_{E0}$  emitter window width and length

 $b_E$ ,  $l_E$  effective (electrical) emitter width and length

I<sub>T</sub>, i<sub>T</sub> DC and time dependent transfer current of the vertical npn transistor structure

I<sub>CK</sub> critical current (indicating onset of high-current effects)

 $\mu_n$ ,  $\mu_p$  electron (hole) mobility

N<sub>Ci</sub> (average) collector doping under emitter

N<sub>Cx</sub> collector doping under external base

Q<sub>p</sub> hole charge

 $\tau_f$  forward transit time

w<sub>B</sub> ,w<sub>B0</sub> neutral/metallurgical base width

w<sub>Ci</sub> (effective) collector width under emitter

w<sub>Cx</sub> (effective) collector width under external base

w<sub>i</sub> width of collector injection zone (for charge storage calculation in collector region)

EC equivalent circuit

GICCR Generalized Integral Charge-Control Relation

SGPM SPICE Gummel-Poon model

HICUM/L0 Introduction

#### 1 Introduction

Advanced standard models like HICUM/L2 [1], MEXTRAM [2] and VBIC [3] eliminate many of the deficiencies of the SPICE Gummel-Poon (SGPM) model. However, these advanced models are also more complicated than the SGPM with respect to the equivalent circuit (EC), model equations, parameter extraction and computational effort. Hence a simplified model has been of high interest to the circuit design community, especially in view of simulations of larger circuits. Hence, HICUM/L0 has been developed [4, 5, 1], which is a simplified version of HICUM/L2 and falls into the same class as the SGPM in terms of simplicity of the equivalent circuit (EC) and element equations, but eliminates the long-standing deficiencies of the SGPM for more advanced process technologies including HBTs. As a result, HICUM/L0 contains improved and more physics-based model equations compared to the SGPM, which also reduces the parameter extraction effort for single (geometry) devices. By offering HICUM/L0, the following issues are being addressed:

- For circuit design, it is often advantageous to start with a simple transistor model that is easily
  understandable for the designer and enables quick hand calculations, but contains the essential
  features of the transistor behaviour. This enables a quick evaluation of the basic circuit functionality, before the time for a longer optimization cycle is spent, using a more accurate model.
- Not all transistors in a larger circuit need to be modelled with a full HICUM/L2 version. In fact, there are often only few very critical transistors, for which a sophisticated and very accurate model is required that takes into account all relevant physical effects. Another example are variable capacitors (varactors) that are often realized by transistors, but can be described by simple transistor models. Therefore, by offering a simplified model, simulation time can be reduced. To take full advantage of the speed improvement, HICUM/L0 should be implemented as a separate model rather than as a derivative of the HICUM/L2 using conditional programming.
- Sometimes, parameter determination for a "single geometry transistor", such as a discrete device, is requested. The extraction methodology for integrated circuit design, however, relies on devices with multiple geometries and certain test structures, which are not available in this case. As a consequence, less information on the transistor is available and, therefore, only a smaller number of parameters and EC elements can be extracted independently. For example, geometry scaling cannot be established from measurements of a single device, therefore, not allowing any scalability of the model. The simple EC of HICUM/L0 and the simplified model equations with a reduced number of parameters, address this issue.

Despite the simplifications, HICUM/L0 still meets the following requirements:

• Its parameters can be generated from the process technology specific HICUM/L2 parameter set (used in, e.g., the TRADICA program [6]). Thus, in case of integrated circuit design, no extra effort is required for parameter extraction. A L0 library can be generated automatically from specific data. Alternatively, L0 parameters can also be extracted for a given single device. The first option is the preferred way since the same basic data are used for both L0 and L2.

HICUM/L0 Introduction

 The model equations are as physical as the simplified EC allows, enabling statistical design for larger circuits.

• The model keeps similarities to the standard SGPM many circuit designers are familiar with. However, in contrast to the SGPM, a clear documentation of both the physical background of the model and the definition of model parameters is given, providing modelling and design engineers with the often missing, but required, information on fundamental model limitations.

The major disadvantage of a model simplification is a reduction of the validity range, caused by either inaccurate equations or completely missing physical effects. However, the purpose of a simplified model is to enable circuit designers to quickly obtain a feel for the circuit behaviour by speeding up circuit simulation. The obtained results should always be verified by simulating with the more sophisticated HICUM/L2. In particular, HICUM/L0 *does not include* the following features (compared to HICUM/L2):

- Noise correlation between the transfer current and the dynamic base current.
- Lateral NQS effects, i.e. dynamic emitter current crowding.
- A substrate (coupling) network.
- A bias independent collector-substrate perimeter capacitance (associated, e.g., with a deep trench).
- Both the strong avalanche effect: (voltage dependence at low collector current densities up to  $BV_{CBO}$ ) and a current dependent impact ionization in the BC space-charge region.
- Bias dependent vertical NQS effects and a second-order differential equation for the delay of the transfer current (i.e. no magnitude reduction of the terminal transconductance at high frequencies).

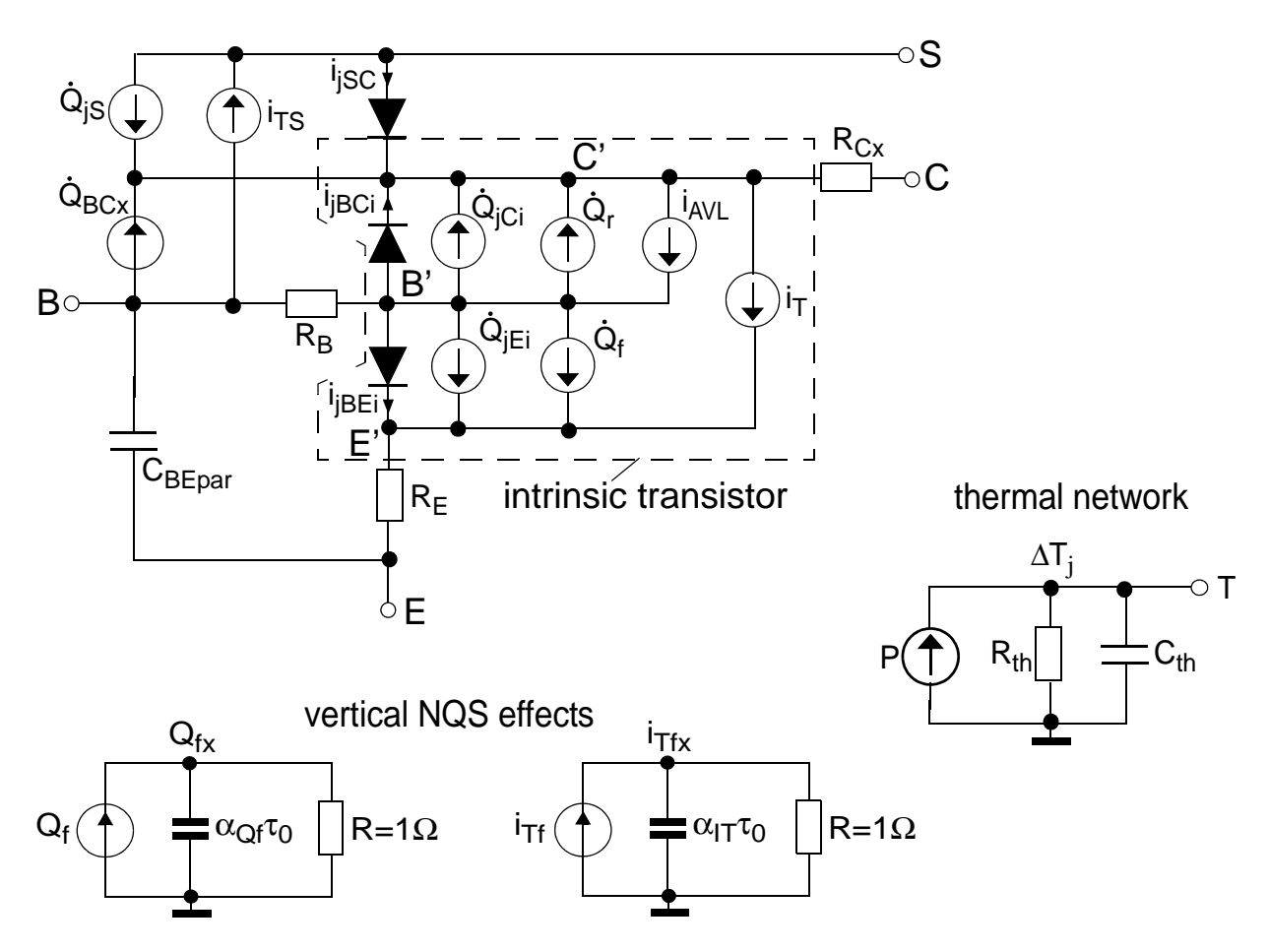
It is to be emphasized that, HICUM/L0 is an independent model combining the simplicity of the SGPM with some important features of HICUM/L2. Detailed derivations and the physical background of its equations can be found in [1]. HICUM/L0 is being implemented in Verilog-A and has been made available for commercial circuit simulators.

The previous and current L0 documents and codes are available at [23].

## 2 Equivalent circuit

The equivalent circuit (EC) of HICUM/L0 is shown in Fig 2.0.0/1. It results from the HICUM/L2 EC by merging elements and neglecting certain physical effects [1]. Thus the EC of the internal, peripheral and external transistor regions cannot be clearly distinguished any more. The partial loss of direct physical correspondence is a result of the simplification.

It is recommended to make the thermal node accessible to the outside in a simulator implementation in order to allow modelling of thermal coupling through distributed thermal networks.



<u>Fig. 2.0.0/1:</u> Complete large-signal equivalent circuit of HICUM/L0 with core electrical EC and adjunct networks for self-heating (thermal network) and vertical non-quasi-static effects for mobile charge and transfer current.

#### 2.1 Model formulation overview

Compared to HICUM/L2, the following simplifications have been made in the EC topology.

• The perimeter base node (B\*) has been eliminated by properly merging the respective internal and external component of the BE depletion capacitance  $C_{jE}$ , base resistance  $r_B$ , base current  $i_{jBE}$  across BE junction, and of the BC depletion capacitance  $C_{jC}$ .

• The BE tunnelling current, the substrate coupling network, the parasitic substrate transistor, and the capacitance for modelling AC emitter current crowding have been omitted.

The resulting isothermal EC is the same as for the SGPM, except for the

- current i<sub>AVI</sub> representing the BC weak avalanche effect;
- parasitic capacitance elements,  $C_{BEpar}$  and  $C_{BCpar}$  (included in the element  $\dot{Q}_{BC}$ ), that result from fringing fields in isolation regions;
- self-heating network, consisting of the generated power P as well as the thermal resistance  $R_{th}$  and capacitance  $C_{th}$ ;
- adjunct network for modelling the vertical NQS effect of the mobile charge in order to ensure a correct excess phase of the current and power gain;

Furthermore, compared to the SGPM, various physical effects are taken into account or are formulated in an improved form in the model equations for the various elements.

A main feature of HICUM/L0 is the decoupling of d.c and a.c behaviour which on one hand makes parameter extraction easier for single devices but on the other hand reduces the validity range of the model and the relation to device physics. Below, the charge equations of the internal transistor are described first, followed by the formulation of the transfer current. After that, equations of the various other elements of the equivalent circuit are discussed.

## 2.2 Depletion charges and capacitances

Modelling of the bias dependence of the depletion charges  $(Q_j)$  and capacitances  $(C_j)$  follows the equations given for HICUM/L2. The mapping equations for the merged elements and differences to HICUM/L2 are discussed below.

## 2.2.1 Base-emitter junction

Compared to HICUM/L2, the BE depletion capacitance components of the internal and peripheral transistor are merged into a single element,

$$C_{jE} = C_{jEi} + C_{jEp} ,$$

using also merged values for the zero-bias capacitance  $C_{jE0}$ , the built-in voltage  $V_{DE}$ , the exponent coefficient  $z_E$  and the ratio  $a_{jE} = C_{jE,max}/C_{jE0}$ . The form of the classical expressions for the BE depletion charge remains the same as in the previous model version. However, the auxiliary voltage  $v_j$  has now been replaced by a *hyperbolic* smoothing expression,

$$v_j = V_f - V_T \frac{x + \sqrt{x^2 + a_{fj}}}{2} < V_f$$
 (2.2.1-1)

using the argument

$$x = \frac{V_f - v_{B'E'}}{V_T} \ . \tag{2.2.1-2}$$

 $V_f$  is the voltage at which at large forward bias the capacitance of the classical expression intercepts the maximum constant value  $a_{iE}C_{iE0}$  [1],

$$V_f = V_{DEi}[1 - a_{jEi}^{-(1/z_{Ei})}]. (2.2.1-3)$$

In (2.2.1-1), the value of  $a_{fj}$  has been adjusted to yield results equivalent to the former formulation, which gives,

$$a_{fj} = 1.921812 {.} {(2.2.1-4)}$$

It is to be noted that  $a_{fi}$  is not a model parameter, but a fixed constant within the code.

The total capacitance is calculated from the derivative of the charge and consists of a classical portion and a component for high forward bias,

$$C_{jE} = \frac{C_{jE0}}{(1 - v_{j}/V_{DE})^{z_{E}}} \frac{dv_{j}}{dv_{B'E'}} + a_{jE}C_{jE0} \left(1 - \frac{dv_{j}}{dv_{B'E'}}\right),$$

with the derivative of  $v_i$ ,

$$\frac{dv_j}{dv_{BE'}} = \frac{x + \sqrt{x^2 + a_{fj}}}{2\sqrt{x^2 + a_{fj}}} . (2.2.1-5)$$

The corresponding charge equation reads

$$Q_{jE} = \frac{C_{jE0}V_{DE}}{1 - z_E} \left[ 1 - \left( 1 - \frac{v_j}{V_{DE}} \right)^{(1 - z_E)} \right] + a_{jE}C_{jE0}(v_{B'E'} - v_j) .$$

The zero-bias value is directly related to the respective HICUM/L2 values for the internal and peripheral transistor:

$$C_{jE0} = C_{jEi0} + C_{jEp0} .$$

Similarly, the value of  $a_{jE}$  is simply given by  $C_{jE,max} = C_{jEi,max} + C_{jEp,max}$ , i.e.

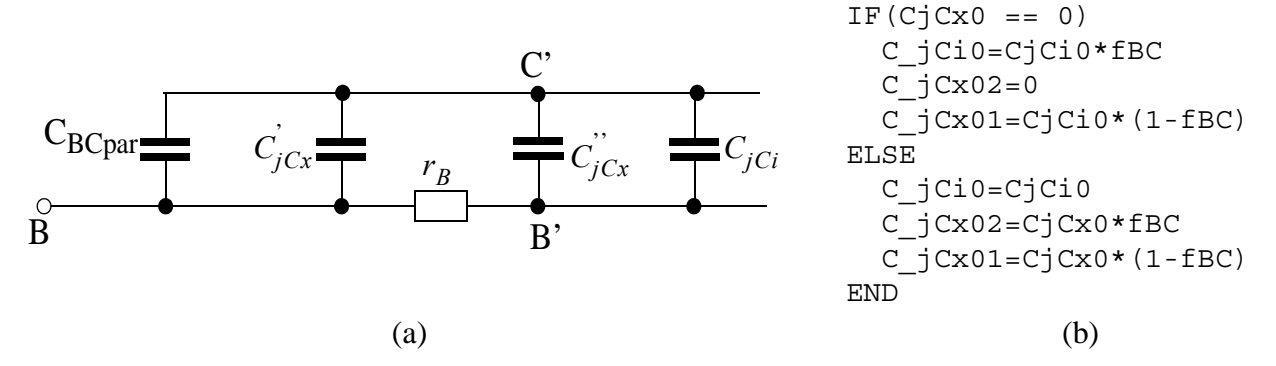
$$a_{jE} = \frac{a_{jEi}C_{jEi0} + a_{jEp}C_{jEp0}}{C_{iE0}} \ .$$

For each transistor configuration, the values of  $V_{DE}$  and  $z_E$  can be extracted from exercising HI-CUM/L2 equations at the appropriate forward bias.

#### 2.2.2 Base-collector junction

Due to the simplified EC, the BC depletion capacitance must now be partitioned across the *total* base resistance. The resulting "internal" and "external" portions have been labelled in Fig. 2.0.0/1 with a star,  $C_{jCi}^*$  and  $C_{jCx}^*$ , in order to distinguish them from the physical components (and values)

used in HICUM/L2. For transistors with a selectively implanted collector, which is a standard option in high-speed processes today, the (original) physical components  $C_{jCi}$  and  $C_{jCx}$ , as they are used in HICUM/L2, differ in their bias dependence, particularly in terms of punch-through behavior. Therefore and in order to provide sufficient flexibility for modelling the high-frequency characteristics, a separate set of model parameters has to be maintained for these elements. This can be done by implementing the BC depletion capacitance as shown in Fig. 2.2.2/1. The internal depletion portion,  $C_{jCi}$ , maintains its separate parameter set. The external depletion capacitance,  $C_{jCx0} = C_{jCx0}^{'} + C_{jCx0}^{''}$ , consists of two elements, split across  $r_{Bx}$  according to a partitioning factor defined by the user. A possible code implementation is shown in 2.2.2/1b, in which  $C_{jCi0}$ ,  $C_{jCx0}$ , and  $f_{BC}$  represent model parameters and the underscored variables are local; the index 1 and 2, respectively, indicate  $C_{jCx0}^{'}$  and  $C_{jCx0}^{''}$ , respectively.



<u>Fig. 2.2.2/1:</u> Implementation of a flexible partitioning scheme for the various BC capacitance components: (a) equivalent circuit; (b) code example.

This implementation not only permits modelling of the internal and external depletion capacitance with *separate* parameters but also provides a simple scheme for partitioning of the total capacitance arbitrarily across  $r_{Bx}$  via adjusting  $f_{BC}$ .

## 2.2.3 Collector-substrate junction

The element  $C_{jS}$  in the EC of Fig. 2.0.0/1 represents the total collector-substrate depletion capacitance, which is modelled by the same formulation as  $C_{jC}$ . In most processes, punch-through is not relevant and the respective parameter can be omitted, which also reduces the computational effort somewhat. The parameters can be directly either measured from capacitance-voltage data or calculated from HICUM/L2.

## 2.3 Minority charges and capacitances

Modelling of the forward transit time and minority charge is based on a simplified version of the HICUM/L2 equations. This allows an easy extraction particularly from single devices at the expense of direct geometry scalability at high current densities.

The formulation of forward minority charge  $Q_f$  is strongly based on the accurate description of the transit time  $\tau_f$ . Like HICUM/L2, the bias dependent transit time consists two components,

$$\tau_f(v_{CE'}, i_{Tf}) = \tau_f(v_{B'C'}) + \Delta \tau_f(v_{CE'}, i_{Tf}),$$
(2.3-1)

which will be discussed below in more detail. The corresponding total mobile charge used in timedomain (transient) analysis is

$$Q_f = Q_{f0} + \Delta Q_{Ef} + \Delta Q_{fh} . {(2.3-2)}$$

#### a) Low current densities

The transit time reads [1]

$$\tau_{f0}(v_{B'C}) = \tau_0 + \Delta \tau_{0h}(c-1) + \tau_{Bfvl} \left(\frac{1}{c} - 1\right), \qquad (2.3-3)$$

with  $c \approx C_{jCi0}^*/C_{jCi}^* = C_{jCi0}/C_{jCi}$ , since the capacitance ratio does not depend on the zero-bias value. The respective forward minority charge is given by

$$Q_{f0} = \tau_{f0} i_{Tf} . {(2.3-4)}$$

## b) Medium and high current densities

The total increase in the (forward) transit time is given by

$$\Delta \tau_f(v_{CE}, i_{Tf}) = \Delta \tau_{Ef} + \Delta \tau_{fh} . \qquad (2.3-5)$$

Neglecting the bias dependent portion of the collector current spreading formulation in HICUM/L2, the additional base charge contribution and the charge contribution from the neutral collector can be lumped together into

$$\Delta \tau_{fh} = \tau_{hcs} \cdot w^2 \left[ 1 + \frac{2I_{CK}}{i_{Tf} \sqrt{i^2 + a_{hc}}} \right], \qquad (2.3-6)$$

with the normalized injection width

$$w(i_{Tf}) = \frac{w_i}{w_C} = \frac{i + \sqrt{i^2 + a_{hc}}}{1 + \sqrt{1 + a_{hc}}}.$$
 (2.3-7)

and the bias dependent variable

$$i = 1 - \frac{I_{CK}}{I_{Tf}}. (2.3-8)$$

The critical current  $I_{CK}$  is described by the same voltage dependence as for HICUM/L2,

$$I_{CK} = \frac{v_{ceff}}{r_{Ci0}^*} \frac{1}{\left(1 + \left(\frac{v_{ceff}}{V_{lim}}\right)^{\delta_{ck}}\right)^{1/\delta_{ck}}} \left[1 + \frac{x + \sqrt{x^2 + a_{ick}}}{2}\right],$$
(2.3-9)

with  $r_{Ci0}^*$  as the (low-field) internal collector resistance, that possibly includes a lumped factor for collector current spreading,  $V_{\text{lim}}$  as the voltage defining the boundary between low and high electric fields in the collector,  $\delta_{ck}$  for a more flexible description of the field dependent mobility in the collector,  $a_{\text{ick}} = 10^{-3}$ ) as a smoothing parameter, and  $x = (v_{\text{ceff}} - V_{\text{lim}})/V_{\text{PT}}$  with  $V_{\text{PT}}$  as epi-collector punch-through voltage. The effective CE voltage is given by

$$v_{ceff} = V_T \left[ 1 + \frac{u + \sqrt{u^2 + 1.921812}}{2} \right]$$
 with the argument  $u = \frac{v_c - V_T}{V_T}$  (2.3-10)

where

$$v_c = v_{CE'} - V_{CE's}$$
 or  $v_c = V_{DCk} - v_{B'C'}$  . (2.3-11)

The internal CE saturation voltage  $V_{\text{C'E's}}$  ( $\approx V_{\text{DEi}}$ - $V_{\text{DCi}}$ ) is a model parameter. From v2.0 on, either one of the above options for  $v_{\text{c}}$  above can be selected by specifying  $V_{\text{DCk}}$  (> 0) regardless of the

value for  $V_{C'E's}$ . Ideally,  $V_{DCk} = V_{DCi}$ , but this couples the critical current modelling with the  $C_{jCi}$  modelling and becomes inaccurate (for  $I_{CK}$ ) especially for a forward biased internal BC junction.

After integrating  $\Delta \tau_{\text{fh}}$  over  $I_{\text{Tf}}$ , the resulting additional charge is then,

$$\Delta Q_{fh} = \tau_{hcs} i_{Tf} w^2 . \qquad (2.3-12)$$

and corresponds to the HICUM/L2 expression with  $f_{thc} = 0$ ; i.e. no collector current spreading.

The emitter component of transit time and charge is given by

$$\Delta \tau_{Ef} = \tau_{Ef0} \left( \frac{i_{Tf}}{I_{CK}} \right)^{g_{\tau E}} \tag{2.3-13}$$

and after integrating  $\Delta \tau_{\rm Ef}$  over  $I_{\rm Tf}$ 

$$\Delta Q_{Ef} = \Delta \tau_{Ef} \frac{i_{Tf}}{1 + g_{\tau E}}. \qquad (2.3-14)$$

The model parameters in the above expression are  $\tau_{hcs}$ ,  $a_{hc}$ ,  $\tau_{fE0}$ ,  $g_{\tau E}$ . The model parameters  $r_{Ci0}$ ,  $V_{lim}$ ,  $V_{PT}$  and  $\{V_{CEs}, V_{DCk}\}$  for the critical current  $I_{CK}$  [8, 9] are the same as in HICUM/L2. Above formulation neglects also the BC barrier effect, which allows merging the base and collector component of into a single expression.

In order to maintain an accurate physics-based description of the shift of the transit time increase with  $V_{C'E'}$  or  $V_{B'C'}$ , temperature, doping and geometry, the bias independent portion of the collector current spreading factor,  $f_{cs}$ , can be included in  $I_{CK}$  via  $r_{Ci0}$  according to [1] and [9]. Together with adjusting the parameter  $\tau_{hcs}$  properly, the impact of possible current spreading on  $\Delta \tau_f$  can then still be included.

The "reverse" transit time  $\tau_r$  is assumed to be bias independent. The corresponding charge is then

$$Q_r = Q_{r0} = \tau_r \, i_{Tr} \,. \tag{2.3-15}$$

Geometry scaling can still be achieved by extracting the parameters of the simplified equations from the full HICUM/L2 formulation.

## 2.4 Simplified transfer current equation

The basic objective is to find an explicit expression for the transfer current which will be simple but sufficiently accurate over the practically utilized bias region up to around  $I_{\rm C}(f_{\rm T,peak})$ . The initial HICUM/L0 version (1.12) exposed a weaknesses of the transfer current formulation [11, 1] for a certain combination of parameters, which has been eliminated from v1.2 on. The resulting simplified transfer current formulation, which completely decouples DC and AC description, is shown below.

$$i_T = i_{Tf} - i_{Tr} = \frac{I_S}{q_{pT}} \left[ \exp\left(\frac{v_{B'E'}}{\boldsymbol{m}_{Cf}V_T}\right) - \exp\left(\frac{v_{B'C'}}{\boldsymbol{m}_{Cr}V_T}\right) \right], \qquad (2.4-1)$$

with the saturation current  $I_S$  and the emission factors  $m_{Cf}$ ,  $m_{Cr}$  as model parameters. Nonlinear non-ideal effects are described by the normalized hole charge

$$q_{pT} = q_j + q_{fl} + \Delta q_{fT}. (2.4-2)$$

Here,

$$q_j = 1 + \frac{v_{jEi, dc}}{V_{Er}} + \frac{v_{jCi}}{V_{Ef}}$$
 (2.4-3)

corresponds to the sum of the simplified normalized zero-bias depletion charges, which are controlled by the voltage functions

$$v_{jEi, dc} = Q_{jEi, dc} / C_{jE0}$$
, (2.4-4)

and

$$v_{jCi} = Q_{jCi}/C_{jCi0}$$
, (2.4-5)

with  $V_{Er}$  and  $V_{Ef}$  as reverse and forward Early voltages, which are the model parameters.

The use of the transfer current related "DC" BE depletion charge  $Q_{\rm jEi,dc}$  as well as the normalization to the zero-bias capacitances and the use of Early voltages decouples the parameter extraction for the transfer current and dynamic transistor behavior. The DC depletion charges are calculated the same way as the actual depletion charges, but with a different parameter set ( $V_{\rm DE,dc}$ ).

 $z_{\rm E,dc}$ ,  $a_{\rm jE,dc}$ ); their values take into account the bias dependent weight factor in the GICCR charge of HICUM/L2. The default (initial) values for  $V_{\rm DE,dc}$ ,  $z_{\rm E,dc}$ ,  $a_{\rm jE,dc}$  can be set to the values of the actual depletion capacitance. Since generally similar accuracy for  $Q_{jEi}$  can be obtained with different value pairs for ( $V_{\rm DEi,dc}$ ,  $z_{\rm Ei,dc}$ ), it is recommended to keep  $z_{Ei}$ ,  $dc = z_{Ei}$  and to only use  $V_{\rm DEi,dc}$  and  $a_{\rm jEi,dc}$  as parameter. For the forward Early effect, the internal BC depletion charge can be used directly, since the corresponding parameters can be specified as model parameters.

The normalized low-injection mobile charge

$$q_{fl} = \frac{i_{Tfi}}{I_{Of}(v_{B'C'})} + \frac{i_{Tri}}{I_{Or}}$$
 (2.4-6)

is defined via a current independent transit time. The current  $I_{Or}$  is a model parameter, while

$$I_{Qf}(v_{B'C'}) = \frac{I_{Qf}}{1 + f_{iqf} \left[ \frac{\tau_{f0}(v_{B'C'})}{\tau_0} - 1 \right]}.$$
 (2.4-7)

Here,  $I_{Qf}$  and  $f_{iqf}$  are model parameters. The latter acts as flag that allows to entirely deactivate the voltage dependence. Physically, the two currents  $I_{Qf}$  and  $I_{Qr}$  represent base conductivity modulation, if for  $\tau_{f0}$  just the base transit time would be inserted.

Finally,

$$\Delta q_{fT} = \left( w^2 (i_{Tf}) + t_{fh} \frac{i_{Tfl}}{I_{CK}} \right) \frac{i_{Tfl}}{I_{Qfh}}$$
 (2.4-8)

represents the simplified current and BC voltage dependent mobile charge at high injection, with the two model parameters  $I_{Ofh}$  and  $t_{fh}$ . Furthermore,

$$i_{Tfl} = \frac{i_{Tfl}}{q_{pT,l}}$$
 and  $i_{Trl} = \frac{i_{Trl}}{q_{pT,l}}$  (2.4-9)

are the *low-injection approximations* of the forward and reverse transfer current components, which are calculated from the normalized *low-injection* hole charge,

$$q_{pT,l} = \frac{q_j}{2} + \sqrt{\left(\frac{q_j}{2}\right)^2 + q_{fl}},$$
 (2.4-10)

and the ideal current components,

$$i_{Tfi} = I_S \exp\left(\frac{v_{B'E'}}{m_{Cf}V_T}\right) \text{ and } i_{Tri} = I_S \exp\left(\frac{v_{B'C'}}{m_{Cr}V_T}\right).$$
 (2.4-11)

Note that  $q_{pT,l}$  results from the solution of a quadratic equation with  $q_j$  from (2.4-3) and  $q_{fl}$  from (2.4-6). According to (2.4-1) and (2.4-11) the transfer current components read,

$$i_{Tf} = \frac{i_{Tfi}}{q_{pT}} = \frac{i_{Tfl}}{1 + \frac{\Delta q_{fT}(i_{Tfl})}{q_{pT,l}}} \quad \text{and} \quad i_{Tr} = \frac{i_{Tri}}{q_{pT}} = \frac{i_{Trl}}{1 + \frac{\Delta q_{fT}(i_{Tfl})}{q_{pT,l}}}.$$
 (2.4-12)

The above solution was implemented in version1.12.

With certain parameter combinations, above solution can lead to a negative transconductance over a small bias range at high current densities. The corresponding details can be found in [11, 1]. The problem can be circumvented by defining the charge variables

$$\Delta q_{BCfi} = \frac{w^2(q_{pT})}{I_{Qfh}} i_{Tfi}$$
 and  $\Delta q_{Efi} = t_{fh} \frac{i_{Tfi}^2}{I_{CK}I_{Qfh}}$ , (2.4-13)

and inserting them into (2.4-8) so that (2.4-2) becomes the third-order equation

$$q_{pT}^{3} - q_{j}q_{pT}^{2} - q_{fl}q_{pT} - \Delta q_{BCfi}(q_{pT})q_{pT} - \Delta q_{Efi} = 0, \qquad (2.4-14)$$

which can be solved using *Cardano's approach* with respect to  $q_{pT}$  (cf. Appendix). The results are shown in Fig. 2.4.0/1, where a comparison between HICUM/L2 and HICUM/L0 is shown. Here, high current effects were turned off in both models and  $g_{\tau/E}$ =1 was used in L2. This case was used, since it represents exactly the preconditions for an analytical solution. As shown, transfer current and transconductance of L0 perfectly match those of L2. Here, the ratio  $t_{fh}/I_{Qfh}$  was directly calculated from L2 parameters.

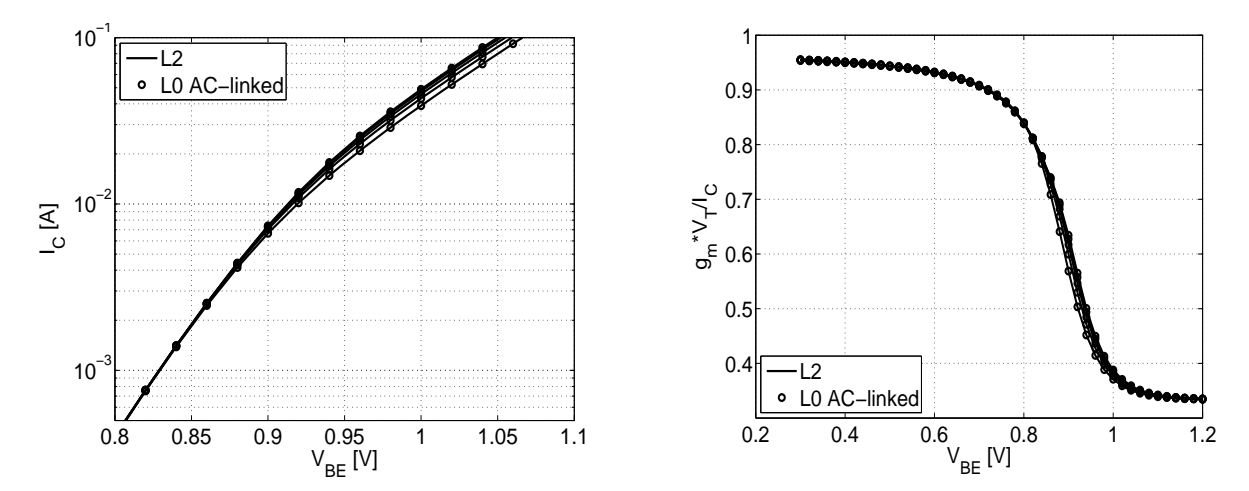


Fig. 2.4.0/1: $I_C$  and  $g_m$  for reference temperature using Cardano's equations (set  $g_{\tau fe}$ =1 in HICUM/L2 model, to show the usability of the equations). No influence of high current effects ( $\tau_{hcs}$ =0 and  $I_{qfh}$  very large). Results shown for various  $V_{BC}$ .

In summary, in HICUM/L0  $q_{pT}$  is calculated three times. The calculation of the collector related minority charge has not been changed. There,  $q_{pT}$  is calculated first with w=0 and then with w=1. These results are used to calculate the final value for w. In order to reduce the computational effort, only the final  $q_{pT}$  is calculated as third order polynomial. Both intermediate values are still calculated as in the previous version. This results in a more generalized form for the HICUM/L0 transfer current.

$$i_{Tf} = \frac{I_{s}}{q_{j} + \frac{i_{Tf}}{I_{CKf}} + \frac{i_{Tr}}{I_{CKr}} + w^{2} \frac{i_{Tf}}{I_{Qfh}} + \left(\frac{i_{Tf}}{I_{CK}}\right) \frac{i_{Tf}}{I_{QfE}}}$$
(2.4-15)

This approach may lead to some simplifications in the parameter extraction.

Finally,  $t_{fh}$  can simply be calculated by

$$t_{fh} = \frac{I_{Qfh}}{I_{QfE}}. (2.4-16)$$

For more details see [15].

#### 2.4.1 Low and medium current density range

Since HICUM/L2 has been extended to a bias dependent weight factor  $h_{jEi}$  [14], the same equations can be used for  $V_{Er}$ , leading to a bias dependent parameter

$$V_{Er} = V_{Er0} / \left(\frac{\exp(u) - 1}{u}\right)$$
 (2.4-1)

with

$$u = a_{VEr} \left( 1 - \left( 1 - \frac{v_{j,u}}{V_{DE}} \right)^{z_E} \right)$$
 (2.4-2)

Here,  $V_{Er0}$  is the Early voltage for zero volt and  $a_{VEr}$  the parameter describing the change of the Early voltage. Towards and beyond  $V_{DE}$ , the voltage  $v_{B'E'}$  is limited smoothly by

$$v_{j,u} = V_{DE} - r_{VEr} V_T \frac{x_u + \sqrt{x_u^2 + a_{fi}}}{2}$$
 with  $x_u = \frac{V_{DE} - v_{B'E'}}{r_{VEr} V_T}$ , (2.4-3)

with the model parameter  $r_{VEr}$  and the smoothing constant  $a_{fi}$ = 1.921812. A possible division by zero in the Bernoulli function  $B(u) = [\exp(u) - 1]/u$  in (2.4-1) at  $v_{B'E'}$ =0 is avoided by a series expansion and with the following implementation:

$$B(u) = \begin{cases} \frac{\exp(u) - 1}{u} & \text{for } |u| \ge u_{min} \\ 1 + \frac{u}{2} & \text{for } |u| < u_{min} \end{cases}.$$
 (2.4-4)

The boundary for the series expansion has been set to  $u_{\min} = 0.001$  and is not critical since  $1/V_{Er}$  is multiplied with a vanishing (normalized) BE depletion charge in the corresponding bias region.

The parameters  $V_{DE}$  and  $z_E$  used here are the same as for the electrostatic capacitance. For simplification, the parameter  $r_{VEr}$  is set to a fixed value of two (2), which can be shown to be sufficient for all verifications [15]. The bias dependence of  $V_{Er}$  can be turned off by settings  $a_{VEr}$  to zero.

#### 2.4.2 High current densities

In HICUM/L2 model, the range of medium currents was extended by a weight factor  $h_{f0}$ . However, any changes for  $I_{Qf}$  (except for temperature dependences) are not necessary, since  $I_{Qf}$  is itself a model parameter so it could be set to any value. The equation to calculate its value from HICUM/ L2 parameters can be written as,

$$I_{Qf} = \frac{Q_{p0}}{h_{f0}\tau_{f0}}.$$

Since v1.3.1, the third order polynomial function of the transfer current at high injection (resulting from  $g_{\tau/E}=1$  in HICUM/L2) has been solved directly.

# 2.5 Static base current components

## 2.5.1 Injection across the BE junction

The components resulting from back injection into the emitter across the *perimeter* and *bottom* BE junction are merged into a single diode,

$$i_{jBE} = I_{BES} \left[ \exp\left(\frac{v_{B'E'}}{m_{BE}V_T}\right) - 1 \right] + I_{RES} \left[ \exp\left(\frac{v_{B'E'}}{m_{RE}V_T}\right) - 1 \right],$$

consisting of a (usually almost) ideal and a (non-ideal) recombination component. The saturation currents and ideality coefficients are model parameters, that allow to model the base current independently of the collector current. Thus in contrast to the SGPM, the current gain - although a useful parameter for circuit design, has been eliminated as model parameter to have a flexible and accurate model formulation.

The saturation currents follow from HICUM/L2 parameters as:

$$I_{BES} = I_{BEiS} + I_{BEpS}$$
 and  $I_{RES} = I_{REiS} + I_{REpS}$ .

If a constant current gain  $B_f$  in the relevant collector current region is desired by the designer, the model parameters have to be set as follows:

$$I_{BES} = I_{CS} / B_f$$
 and  $m_{BE} = m_{Cf}$ .

#### 2.5.2 Injection across the BC junction

The diode current  $I_{iBC}$  injected into the collector across the BC junction, is described by:

$$i_{jBC} = I_{jBCS} \left[ \exp\left(\frac{v_{B'C}}{m_{BC}V_T}\right) - 1 \right].$$

Usually, this current is negligible but it provides a d.c path between the nodes B' and C', which sometimes aids convergence and also can be regarded as flag for designers if the transistor enters an undesired operating region outside the model's validity range.

#### 2.5.3 Avalanche current

In HICUM/L2, the *weak* avalanche current is modelled as [1, 7],

$$i_{AVL} = i_{Tf} \frac{f_{AVL} V_{DCi}}{C_c^{1/z_{Ci}}} \exp \left( -\frac{q_{AVL}}{C_{jCi0} V_{DCi}} C_c^{\left(\frac{1}{z_{Ci}} - 1\right)} \right),$$

with  $C_c = C_{iCi}(v_{B'C'})/C_{iCi0}$ , and the avalanche factors

$$f_{AVL} = 2a_n/b_n$$
 and  $q_{AVL} = b_n \varepsilon A_E/2$ ,

which depend on emitter area, physical data and temperature (via  $a_n$  and  $b_n$ ). Here  $a_n$  and  $b_n$  are the (temperature dependent) ionization coefficients. The two model parameters  $f_{AVL}$  and  $f_{AVL}$  can be taken over from HICUM/L2.

#### 2.5.4 Injection across the collector-substrate junction

Depending on the transistor structure and layout and electrical conditions, a parasitic substrate transistor can be turned on. The transfer current of which can be expressed as,

$$I_{TS} = I_{TSS} \left[ \exp\left(\frac{v_{B'C}}{m_S V_T}\right) - \exp\left(\frac{v_{S'C}}{m_S V_T}\right) \right]$$
 (2.5-1)

It is to be noted that, the same non-ideality coefficient is being used for forward and inverse operation of the substrate transistor.

The total current across the collector substrate junction is described by the usual diode equation:

$$i_{jSC} = I_{SCS} \left[ \exp\left(\frac{v_{SC}}{m_{SC}V_T}\right) - 1 \right].$$

The diode aids d.c convergence; in addition, a conducting diode is a good indication for designers that the transistor enters an undesired operating region.

## 2.6 Internal base resistance

Starting point for the L0 model is the description of the DC internal base sheet resistance in HI-CUM/L2,

$$\frac{1}{q_{rb}} = \frac{r_{SBi}}{r_{SBi0}} = \frac{1}{1 + \frac{Q_{jEi} + Q_{jCi}}{Q_{rb0}} + \frac{Q_f + Q_r}{Q_{rb0}}},$$
(2.6-1)

with  $q_{rb}$  as the normalized charge,  $r_{SBi0}$  as the zero bias sheet resistance, and

$$Q_{rh0} = Q_{r0} + \Delta Q_{rh0} = (1 + f_{DQr0})Q_{r0} \ge Q_{r0}, \qquad (2.6-2)$$

as modified "zero-bias" charge due to mobility changes with bias [15]. Since the actual values of the internal junction charges are not separately available in HICUM/L0, the corresponding charge ratios has to be replaced by available quantities.

At low current densities, the internal base sheet resistance is only voltage dependent via the depletion charge ratio. Normalizing the latter to their zero-bias capacitance, that is defining  $q_j = Q_j / C_{j0}$ , the charge ratio is approximated here by

$$\frac{Q_{jEi} + Q_{jCi}}{Q_{rb0}} \cong \frac{v_{jE}}{V_{r0E}} + \frac{v_{jCi}}{V_{r0C}} , \qquad (2.6-3)$$

with the voltage function  $v_{jE} = Q_{jE} / C_{jE0}$  and  $v_{jCi} = Q_{jCi} / C_{jCi0}$ . Furthermore,  $V_{r0E} = Q_{rb0} / C_{jE0}$  and  $V_{r0C} = Q_{rb0} / C_{jCi0}$  are model parameters, which are defined similarly to the artificial Early-voltages used for  $i_{Tf}$ .

In analogy to the simplification of the current dependent charge ratios for the (G)ICCR, the ratio containing the minority charges in (2.6-1) can be simplified by introducing "critical" currents  $I_{rBif}$  and  $I_{rBif}$ ,

$$\frac{Q_f + Q_r}{Q_{rb0}} \cong \frac{I_{Tf}}{I_{rBif}} + \frac{I_{Tr}}{I_{rBir}} , \qquad (2.6-4)$$

with  $I_{rBif} = Q_{rb0}/\tau_{f0}$  and  $I_{rBir} = Q_{rb0}/\tau_{r}$ . Since HICUM/L0 becomes less accurate at high current densities, the number of model parameters is further reduced by setting  $I_{rBif} = I_{Qf}$  and  $I_{rBir} = I_{Qr}$ .

Defining,

$$Q_{z} = \left(1 + \frac{v_{jE}}{V_{r0E}} + \frac{v_{jCi}}{V_{r0C}} + \frac{I_{Tf}}{I_{Qf}} + \frac{I_{Tr}}{I_{Qr}}\right), \qquad (2.6-5)$$

the internal base resistance that results from conductivity modulation only is therefore given by

$$r_i = \frac{r_{Bi0}}{f_{Qz}}, \qquad (2.6-6)$$

where,

$$f_{Qz} = \frac{1}{2} \left\{ Q_z + \sqrt{Q_z^2 + 0.01} \right\}, \qquad (2.6-7)$$

is a smoothing function to avoid a divide by zero at too large reverse bias.  $r_{Bi0}$  is a model parameter, that is a function of zero-bias sheet resistance  $r_{SBi0}$  and emitter configuration (i.e. number of emitter and base fingers) [16].

The effect of emitter current crowding can in general be described by the function [16]

$$\psi(\eta) = \frac{\ln(1+\eta)}{\eta} , \qquad (2.6-8)$$

with the current crowding factor

$$\eta = f_{geo} \frac{r_i I_{BE}}{V_T} \,, \tag{2.6-9}$$

which depends on the sheet resistance  $r_{SBi0}$ , the internal base current and emitter geometry via the factor  $f_{geo}$ . Due to the model simplifications, the internal base current  $(I_{BEi})$  is not directly available so that  $\eta$  has to be calculated from the total base current  $I_{BE} = I_{BEi} + I_{BEp}$ . This is done by modifying the geometry factor  $f_{geo}$  to

$$f_{geo}^* = \frac{f_{geo}}{1 + \gamma_B (P_{EO}/A_{EO})} , \qquad (2.6-10)$$

which now contains the base current bottom-to-perimeter partitioning at low current densities and can be calculated from HICUM/L2 parameters. As a result

$$\eta = f_{geo}^* \frac{r_i I_{BE}}{V_T} \,. \tag{2.6-11}$$

Note that  $f_{geo}^*$  does not depend on bias and, therefore, is a model parameter that can be directly extracted for a given (transistor) geometry.

The final equation for the internal base resistance then reads

$$r_{Bi} = r_i |\psi(\eta)|, \qquad (2.6-12)$$

and contains the model parameters  $r_{Bi0}$ ,  $V_{r0E}$ ,  $V_{r0C}$  and  $f_{geo}^*$ .

For circuit design, often an estimation of the internal base resistance close to the circuit operation is of interest. The low-current value of  $r_{Bi}$  can be roughly approximated using simple voltage ratios like in the SGPM:

$$\frac{r_{SBi}}{r_{SBi0}} = \frac{1}{1 + \frac{v_{B'E}}{V_{rBif}} + \frac{v_{B'C}}{V_{rBir}}},$$
(2.6-13)

with  $V_{rBif}$  and  $V_{rBir}$  as constants. For instance,  $V_{rBif}$  can be estimated as the ratio  $V_{r0E}/c_{jE,op}$  with the model parameter  $V_{r0E}$  and the normalized capacitance  $C_{jE,op}$  at the desired bias value.

#### 2.7 External series resistances

The equivalent circuit of Fig. 2.0.0/1 contains the operating point independent series resistances for the external collector region,  $r_{Cx}$ , and for the emitter region,  $r_E$ . In contrast to HICUM/L2, the EC contains only a single base resistance element representing the *total* base resistance

$$r_B = r_{Bi} + r_{Bx} . (2.7-1)$$

The physical meaning of all series resistor components is the same as for HICUM/L2.

Since in the simplified EC the internal base resistance cannot be accessed anymore through a separate node (between  $r_{Bx}$  and  $r_{Bi}$ ) the *lateral NQS effect* (i.e. dynamic emitter current crowding) is omitted in HICUM/L0.

## 2.8 External (parasitic) capacitances

In addition to the junction and diffusion capacitances, both of which are bias dependent, advanced processes contain constant capacitances, that are caused by isolation regions between base, emitter, and collector. In order to make HICUM/L0 applicable for an as large as possible variety of technologies, the corresponding two capacitance elements  $C_{BEpar}$  and  $C_{BCpar}$  have been added to the equivalent circuit of Fig. 2.0.0/1. The capacitances can include also contributions from the metalization above the silicon surface. The values are usually the same as for  $C_{BEpar}$  and  $C_{BCpar}$  HICUM/L2.

# 2.9 Non-quasi-static effects

Non-quasi-static (NQS) effects are occurring at high-frequencies or fast switching processes. Note that the designation "high" or "fast" is relative and depends on the technology employed. NQS effects exist in both vertical and horizontal direction.

Regarding vertical direction, it is a well known fact that at high frequencies minority charge and transfer current are reacting delayed w.r.t the voltage across both pn-junction. While an amplitude change is negligible until about a third of the internal  $f_T$ , a significant phase shift is felt already at  $f_T$  and below. *Vertical NQS effects* are taken into account in HICUM/L0 by additional delay times for both minority charge *and* the transfer current in form of a single-pole low-pass, giving for the ratio of delayed vs. quasi-static dynamic base current component in frequency domain

$$\frac{Q_{f, nqs}}{Q_f} = \frac{1}{1 + j\omega\tau_{Qf}}.$$
(2.9-1)

with the bias independent delay time

$$\tau_{Qf} = \alpha_{Qf} \tau_0. \tag{2.9-2}$$

The frequency dependence of the collector terminal current is, in contrast to HICUM/L2, modelled by a single-pole RC-network, giving for the ratio of delayed vs. quasi-static transfer current

$$\frac{i_{T, nqs}}{i_T} = \frac{1}{1 + j\omega \tau_{IT}}$$
 (2.9-3)

with the bias independent delay time

$$\tau_{IT} = \alpha_{iT} \tau_0. \tag{2.9-4}$$

Eq. (2.9-1) and (2.9-3) are included using RC subcircuits as shown in Fig 2.0.0/1 that enable a consistent description of NQS effects in both frequency and time domain.

The model parameters here are the same as in HICUM/L2:  $\alpha_{Qf}$ ,  $\alpha_{iT}$  and flnqs. The flag flnqs allows to turn on or off vertical NQS effects without having to change the model parameters.

For more details on NQS effects see [1].

## 2.10 Self-heating

As shown in Fig 2.0.0/1, a simple thermal network for modelling self-heating is provided, consisting of the temperature dependent thermal resistance

$$R_{th}(T) = R_{th}(T_0)[1 + \alpha_{Rth}\Delta T] \left(\frac{T}{T_0}\right)^{\zeta_{Rth}}$$
(2.10-5)

with the model parameters  $\alpha_{Rth}$  and  $\zeta_{Rth}$ , and a temperature independent thermal capacitance  $C_{th}$ . For FLSH=1 (self-heating turned on), the power dissipation is calculated as

$$P = I_{\rm T} V_{\rm C'E'} + I_{\rm AVL} (V_{DCi} V_{\rm B'C'}).$$
 (2.10.0-6)

The temperature node (not the ground node) needs to be accessible to the external circuit for enabling modelling of thermal coupling.

# 2.11 Temperature dependence

The temperature dependent modelling in HICUM/L0 follows closely the equations of HICUM/L2, therefore, attempting to maintain an as strong as possible relation to physics despite simplifications in model equations. In the following formulas,  $T_0$  is the reference temperature for which the model parameters have been determined. The formulas are valid roughly for a temperature range between about 250K and 400K, although this range depends somewhat on the technology considered.

In order to allow simulations of devices fabricated in different materials and to make the model simulator-independent, a temperature dependent bandgap voltage has been added to the model equations. The formulation suggested in [18] has been selected,

$$V_g(T) = V_g(0) + K_1 T \ln(T) + K_2 T , (2.11-1)$$

the main advantages of which are

- a higher accuracy w.r.t measured data in the relevant temperature range compared to the classical formulation, and
- compatibility with existing temperature dependent current formulations in compact models that are based on the assumption of a simple linear temperature dependence  $V_g(T) = V_{g,cl}(0) a_g T$ , but higher accuracy at the same time.

The original coefficient values are given in Table 2.11.0/1; the second row contains an improved set of parameters which is more accurate at low temperatures with respect to the classical formulation

$$V_g(T) = V_{g, cq}(0) - \frac{\alpha_g T^2}{T + T_g}.$$
 (2.11-2)

Parameter	K <sub>1</sub> [V/K]	K <sub>2</sub> [V/K]	V <sub>g</sub> (0) [V]
[15]	-8.459 10 <sup>-5</sup>	3.042 10 <sup>-4</sup>	1.1774
[16]	-1.02377 10 <sup>-4</sup>	4.3215 10 <sup>-4</sup>	1.170

Table 2.11.0/1: Coefficients for calculating the bandgap voltage in silicon as a function of temperature from (2.11-1). In the range from 250 to 400K, a smaller error can be obtained by simply setting  $V_g(0)=1.1777V$  in the original parameter set.

For compact model and application purposes, it is sometimes more convenient to re-write above equation in terms of a reference temperature  $T_0$  (e.g. for parameter extraction), which gives

$$V_g(T) = V_g(T_0) + k_1 \frac{T}{T_0} \ln\left(\frac{T}{T_0}\right) + k_2 \left(\frac{T}{T_0} - 1\right) . \tag{2.11-3}$$

with the definitions

$$k_1 = K_1 T_0$$
 ,  $k_2 = K_2 T_0 + k_1 \ln(T_0)$  , (2.11-4)

and the bandgap voltage at the measurement reference temperature,

$$V_g(T_0) = k_2 + V_g(0) . (2.11-5)$$

Fig. 2.11.0/1 shows the temperature dependent bandgap voltage according to (2.11-1) compared to the most popular conventional formulations.

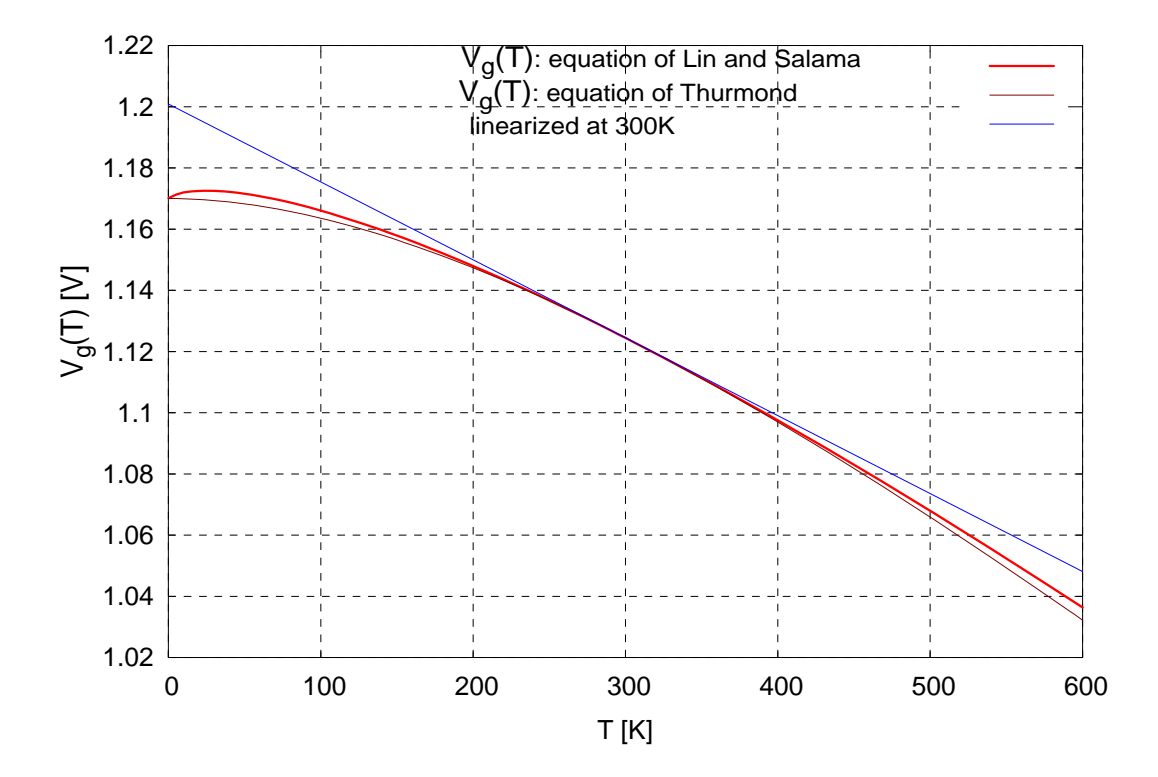


Fig. 2.11.0/1: Comparison of bandgap voltage approximations. The parameters used for (2.11-2) are  $V_g(0) = 1.170 \text{ V}$ ,  $\alpha_g = 4.73 \cdot 10^{-4} \text{ V/K}$ ,  $T_g = 636 \text{ K}$ . The parameters for the (at  $T_0$ ) linearized equation are  $V_g(0) = 1.2009 \text{ V}$ ,  $\alpha_g = 2.5461 \cdot 10^{-4} \text{ V/K}$ .

The choice of the bandgap description also influences the formulation of the effective intrinsic carrier density, which now reads

$$n_{ie}^2(T) = n_{ie}^2(T_0) \left(\frac{T}{T_0}\right)^{m_g} \exp\left[\frac{V_{geff}(0)}{V_T}\left(\frac{T}{T_0} - 1\right)\right],$$
 (2.11-6)

with the constant

$$m_g = 3 - \frac{k_1}{V_{T0}} = 3 - \frac{qK_1}{k_R} , \qquad (2.11-7)$$

and  $K_1$  from the bandgap voltage equation (2.11-1). Using the values in Table 2.11.0/1 for Si gives  $m_g = 4.188$ .

The temperature dependent transfer saturation current is dominated by the intrinsic carrier concentration and given by

$$I_S(T) = I_S(T_0) \left(\frac{T}{T_0}\right)^{\zeta_{CT}} \exp\left[\frac{V_{gb}}{V_T(T)} \left(\frac{T}{T_0} - 1\right)\right],$$
 (2.11-8)

with the bandgap voltage  $V_{Gb}$  (averaged over the base region) and  $\zeta_{CT}$  as model parameters. The saturation currents in the base current components can be written as,

$$I_{BES}(T) = I_{BES}(T_0) \left(\frac{T}{T_0}\right)^{\zeta_{BET}} \exp\left[\frac{V_{ge}}{V_T(T)} \left(\frac{T}{T_0} - 1\right)\right], \qquad (2.11-9)$$

with the new model parameter  $\zeta_{BET}$  and

$$I_{RES}(T) = I_{RES}(T_0) \left(\frac{T}{T_0}\right)^{m_g/2} \exp\left[\frac{V_{gbe}}{2V_T(T)} \left(\frac{T}{T_0} - 1\right)\right],$$
 (2.11-10)

with the  $m_g$  from (2.11-7). Similar equations hold for the junction saturation currents  $i_{BCx}$ ,  $i_{BCi}$  and  $i_{CS}$  of the other diodes, e.g.,

$$I_{BCS}(T) = I_{BCS}(T_0) \left(\frac{T}{T_0}\right)^{\zeta_{BCI}} \exp\left[\frac{V_{gc}}{V_T(T)}\left(\frac{T}{T_0} - 1\right)\right],$$
 (2.11-11)

and

$$I_{SCS}(T) = I_{SCS}(T_0) \left(\frac{T}{T_0}\right)^{\zeta_{SCT}} \exp\left[\frac{V_{gs}}{V_T(T)} \left(\frac{T}{T_0} - 1\right)\right],$$
 (2.11-12)

$$I_{TSS}(T) = I_{TSS}(T_0) \left(\frac{T}{T_0}\right)^{\zeta_{SCT}} \exp\left[\frac{V_{gc}}{V_T(T)} \left(\frac{T}{T_0} - 1\right)\right],$$
 (2.11-13)

with 
$$\zeta_{SCT} = m_g - 1.5$$
, and  $V_{gbe} = (V_{gb} + V_{gc})/2$ .

The temperature dependence of  $I_{Qf}$  is changed [15] according to the new formulations of HI-CUM/L2, which leads to the following expression,

$$I_{Qf}(T) = I_{Qf}(T_0) \left(\frac{T}{T_0}\right)^{\zeta_{IQf}} \exp\left(\frac{-\Delta v_{gBE}}{V_T} \left(\frac{T}{T_0} - 1\right)\right), \qquad (2.11-14)$$

where the *exp-formulation* is added and  $\zeta_{IQF}$  is the temperature coefficient for  $I_{Qf}$  and a model parameter. The corresponding parameter is also used to describe the bias dependence of the reverse Early voltage.

Due to different bandgap voltages in the transistor, high current effects may become also temperature dependent. Since for  $I_{Qfh}$ , minority charges in different regions of the transistor are taken into account, a simple second order polynomial fit is applied [15],

$$I_{Ofh}(T) = I_{Ofh}(T_0)(1 + \alpha_{IOfh}\Delta T + k_{IOfh}\Delta T^2)$$
 (2.11-15)

Temperature dependence of  $t_{fh}$  is expressed as [15],

$$t_{fh}(T) = t_{fh}(T_0) \frac{I_{Qfh}(T)}{I_{Qfh}(T_0)} \exp\left(\frac{v_{gb} - v_{ge}}{V_T} \left(\frac{T}{T_0} - 1\right)\right)$$
(2.11-16)

The temperature dependence of  $t_{ef0}$  is expressed as

$$t_{ef}(T) = t_{ef}(T_0) \left(\frac{T}{T_0}\right)^{\zeta_{tef}} \exp\left(\frac{-(v_{gb} - v_{ge})}{V_T} \left(\frac{T}{T_0} - 1\right)\right),$$
 (2.11-17)

In addition, the flag "flteft" allows to turn on or off the T dependence of  $t_{ef0}(T)$ .

In principle, the bandgap voltages  $V_{gbx}$  and  $V_{gsc}$  differ from  $V_{gb}$  due to the different doping concentrations in the corresponding regions. However, for simplicity reasons

$$V_{gsc} = V_{gbx} = V_{gb} . {(2.11-18)}$$

The temperature dependence of the zero-bias junction capacitances is given by

$$C_{j0}(T) = C_{j0}(T_0) \left(\frac{V_D(T_0)}{V_D(T)}\right)^z. (2.11-19)$$

In addition, the parameter  $a_i$  is modelled temperature dependent as

$$a_j(T) = a_j(T_0) \frac{V_D(T)}{V_D(T_0)}$$
 (2.11-20)

The temperature dependent formulations of the BC avalanche current related parameters read

$$f_{AVL}(T) = f_{AVL}(T_0) \exp(\alpha_{fav}(T - T_0))$$
 (2.11-21)

$$q_{AVL}(T) = q_{AVL}(T_0) \exp(\alpha_{qav}(T - T_0))$$
 (2.11-22)

where  $\alpha_{fav}$  and  $\alpha_{qav}$  are the temperature coefficient of avalanche prefactors. These parameters are the same as for HICUM/L2.

The formulation for the built-in voltages has been extended physically (as in HICUM/L2) to avoid numerical issues at very high temperature. First, an auxiliary voltage is calculated at the reference temperature from the model parameter  $V_D$ ,

$$V_{Dj}(T_0) = 2V_{T0} \ln \left[ \exp \left( \frac{V_D(T_0)}{2V_{T0}} \right) - \exp \left( -\frac{V_D(T_0)}{2V_{T0}} \right) \right], \qquad (2.11-23)$$

with  $V_{T0} = k_B T_0/q$ . Then, the respective value at the actual temperature is calculated,

$$V_{Dj}(T) = V_{Dj}(T_0) \left(\frac{T}{T_0}\right) + V_g \left(1 - \frac{T}{T_0}\right) - m_g V_{T0} \ln\left(\frac{T}{T_0}\right) , \qquad (2.11-24)$$

which corresponds to the classical equation. Finally, the new built-in voltage is calculated as

$$V_D(T) = V_{Dj}(T) + 2V_T \ln \left( \frac{1 + \sqrt{1 + 4\exp(-\frac{V_{Dj}(T)}{V_T})}}{2} \right). \tag{2.11-25}$$

The temperature dependence of low current transit time is given by,

$$\tau_0(T) = \tau_0(T_0)[1 + \alpha_{t0}(T - T_0) + k_{t0}(T - T_0)^2], \qquad (2.11-26)$$

where,  $\alpha_{t0}$  and  $k_{t0}$  are the first- and second-order temperature coefficient of the transit time.

The temperature dependence of reverse Early-voltage is modelled as [15],

$$V_{Er0}(T) = V_{Er0}(T_0) \exp\left[\frac{-\Delta v_{gBE}}{V_T} \left( \left(\frac{T}{T_0}\right)^{\zeta_{vgBE}} - 1 \right) \right]. \tag{2.11-27}$$

Also, the parameter describing the Early-voltage may change due to  $V_T$  and the temperature induced moving of the SCR-boundary. Both effects are modelled using the temperature coefficient

$$a_{VEr}(T) = a_{VEr}(T_0) \left(\frac{T}{T_0}\right)^{\zeta_{VEr}}$$
 (2.11-28)

The temperature dependence expression for the internal collector resistance,

$$r_{Ci0}(T) = r_{Ci0}(T_0) \left(\frac{T}{T_0}\right)^{\zeta_{Ci}},$$
 (2.11-29)

where  $\tau \eta \varepsilon$  temperature coefficient  $\zeta_{Ci}$  of the epi-collector diffusivity is the same as in HICUM/L2.

The temperature dependence for the voltage dividing ohmic and saturation region of the field dependent drift velocity,

$$V_{lim}(T) = V_{lim}(T_0) \left(\frac{T}{T_0}\right)^{(\zeta_{Ci} - \alpha_{vs})},$$
 (2.11-30)

where  $\alpha_{vs}$  is the relative temperature coefficient of the saturation drift velocity.

The CE saturation voltage can be modelled as a linear function of temperature,

$$V_{CEs}(T) = V_{CEs}(T_0)[1 + \alpha_{CEs}\Delta T],$$
 (2.11-31)

with  $\alpha_{\rm CEs}$  as a model parameter. Its value can be estimated from the difference between the respective relative temperature coefficients of the built-in voltages  $V_{\rm DEi}$  and  $V_{\rm DCi}$ . Similarly, the optional parameter  $V_{\rm DCk}$  is modelled as a linear function of temperature according to

$$V_{DCk}(T) = V_{DCk}(T_0)[1 - \alpha_{DCk}\Delta T],$$
 (2.11-32)

with the temperature coefficient  $\alpha_{DCk}$  as model parameter. These formulations are the same as in HICUM/L2.

The temperature dependence of the series resistances is modelled the same way as in HICUM/L2:

$$r_{Cx}(T) = r_{Cx}(T_0) \left(\frac{T}{T_0}\right)^{\zeta_{RCX}},$$
 (2.11-33)

$$r_{Bx}(T) = r_{Bx}(T_0) \left(\frac{T}{T_0}\right)^{\zeta_{RBX}},$$
 (2.11-34)

$$r_{Bi0}(T) = r_{Bi0}(T_0) \left(\frac{T}{T_0}\right)^{\zeta_{RBI}},$$
 (2.11-35)

$$r_E(T) = r_E(T_0) \left(\frac{T}{T_0}\right)^{\zeta_{RE}},$$
 (2.11-36)

where exponent factors  $\zeta_{RCX}$ ,  $\zeta_{RBX}$ ,  $\zeta_{RBI}$  and  $\zeta_{RE}$  are model parameters.

The temperature dependence of the thermal resistance is modelled as

$$R_{th}(T) = R_{th}(T_0) \left(\frac{T}{T_0}\right)^{\zeta_{rth}},$$
 (2.11-37)

with the temperature exponent factor  $\zeta_{rth}$  as model parameter.

## **2.12 Noise**

The (small-signal) noise EC of HICUM/L0 is shown in Fig. 2.12.0/2. It is based on the small-signal model discussed before, but contains in addition for each dissipative element its respective noise source [2]. It is assumed that base and collector current noise sources are uncorrelated.

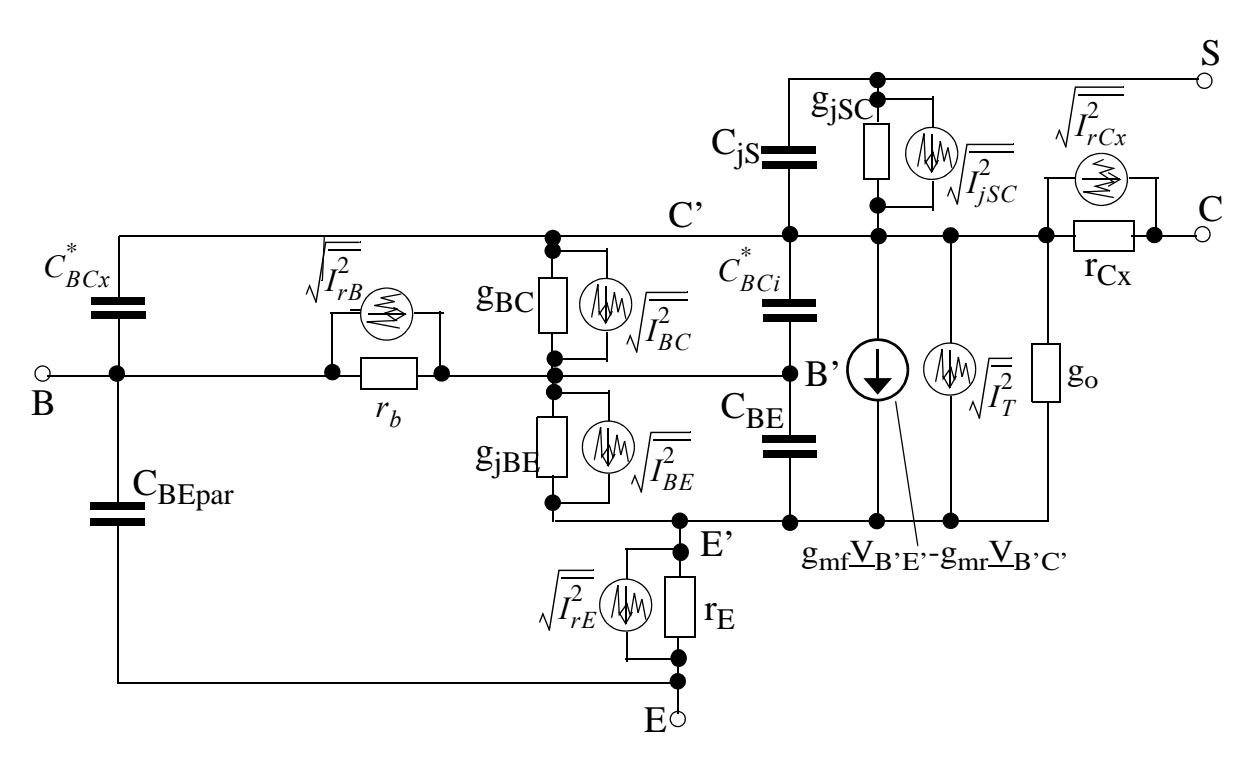


Fig. 2.12.0/2:Small-signal noise equivalent circuit of HICUM/L0, showing the noise sources with their RMS values used in a circuit simulator. The following elements have been merged compared to the small-signal EC in Fig. 2.13.0/1:  $C_{BCx}^* = C_{jCx}^* + C_{BCpar}$ ,  $C_{BCi}^* = C_{jCi}^* + C_{dC}$ ,  $C_{BE} = C_{jE} + C_{dE}$ ,  $g_{BC} = g_{jBC} + g_{AVL}$ .

The various noise (current) sources are described as follows. For series resistors, thermal noise is taken into account,

$$\overline{I_r^2} = \frac{4kT\Delta f}{r} \,, \tag{2.12-1}$$

with  $r = r_E$ ,  $r_{Cx}$  or  $r_B$ .

For the transfer current, shot noise is assumed:

$$\overline{I_T^2} = 2qI_T \Delta f \qquad . \tag{2.12-2}$$

The noise resulting from the current injected across the BE junction into the emitter,

$$\overline{I_{BE}^2} = 2qI_{jBE}\Delta f + k_F I_{jBE}^{a_F} \frac{\Delta f}{f} , \qquad (2.12-3)$$

contains a shot noise and a flicker noise contribution with  $k_F$  and  $a_F$  as the flicker noise model parameters. The currents across the other junctions are assumed to have a shot noise component only,

$$\overline{I_{jdiode}^2} = 2qI_{jdiode} \Delta f , \qquad (2.12-4)$$

with  $diode = \{BC, CS\}.$ 

Noise from avalanche generation within the internal BC depletion region is modelled as shot noise,

$$\overline{I_{AVL}^2} = 2qI_{AVL} \Delta f \quad , \tag{2.12-5}$$

giving for the total noise contribution within the BC junction

$$\overline{I_{BC}^2} = \overline{I_{jBC}^2} + \overline{I_{AVL}^2}$$
 (2.12-6)

HICUM/L0 HICUM/L0 Parameters

# 3 HICUM/L0 Parameters

Below is a reference list of model parameters with a brief description. With the "default" values all but absolutely necessary functions defining a bipolar transistor are turned off. The second parameter set named "test" is being provided for exercising the model with most of the effects being turned on and can be used for model testing.

The factor M allows a scaling of the respective parameters in case of M identical devices connected in parallel.

Table 3.0.0/1:

name	description	default	range	test	unit	factor			
Collector Current									
is	(Modified) saturation current	1E-16	[0:1]	1.35E-18	A	M			
mcf	non-ideality coefficient of for- ward collector current	1.0	(0:10]	1.0	_	-			
mcr	non-ideality coefficient of reverse collector current	1.0	(0:10]	1.0	-	-			
vef	forward Early voltage (nor- malization volt.)	inf	(0:inf]	8.0	V	-			
ver	reverse Early voltage (normalization volt.)	inf	(0:inf]	1.15	V				
a <sub>VEr</sub>	parameter for bias dependence of $V_{Er}$ .	0	[0:100]	0	-	-			
rver	smoothing parameter for ver(VBE) at high voltage	2.0	(0:10]	2.0	-	-			
iqf	forward DC high-injection roll-off current	inf	(0:inf]	3E-2	A	M			
fiqf	flag for turning on voltage dependence of iqf	0	[0:1]	0	-	-			
iqr	inverse DC high-injection roll-off current	inf	(0:inf]	1E6	A	M			
iqfh	high-injection correction current	inf	(0:inf]	1E6	A	М			
tfh	high-injection correction fac- tor	0	[0:inf)	2E-9	-S	-			

HICUM/L0 Parameters

Table 3.0.0/1:

name	description	default	range	test	unit	factor
ahq	smoothing factor for the DC injection width	0	[-0.9:10]	0	-	-
flteft	flag for including (1) or not (0) emitter charge T dependence	0	0 or 1	0	-	-
flitm	switch for different transfer current formulations 0: L0v1.2 solution of second- order equation 1: Cardano (third-order eq.)	0	0 or 1	0	-	-
	Ва	ase Current	t			
ibes	BE saturation current	1E-18	[0:1]	1.16E-20	A	M
mbe	BE non-ideality factor	1	(0:10]	1	-	-
ires	BE recombination saturation current	0	[0:1]	1.16E-16	A	M
mre	BE recombination non-ideality factor	2	(0:10]	2	-	-
ibcs	BC saturation current	0	[0:1]	1.16E-20	A	M
mbc	BC non-ideality factor	1	(0:10]	1.015	-	-
	BE Depl	etion Capa	citance			
cje0	zero-bias BE depletion capacitance	1E-20	(0:inf)	2E-14	F	V
vde	BE built-in voltage	0.9	(0:10]	0.9	V	-
ze	BE exponent factor	0.5	(0:1)	0.5	-	-
aje	ratio of maximum to zero-bias value	2.5	[1:inf)	1.8	-	-
vdedc	BE charge built-in voltage for DC transfer current	0.9	(0:10]	0.9	V	-
zedc	BE charge exponent factor for DC transfer current	0.5	(0:1)	0.5	-	-

# Table 3.0.0/1:

name	description	default	range	test	unit	factor
ajedc	BE capacitance ratio (maximum to zero-bias value) for DC transfer current		2.5	-	-	
	Tr	ansit Time	;			
t0	low current transit time at Vbici=0	0	[0:inf)	5E-12	S	-
dt0h	base width modulation contri- bution	0	(-inf:inf)	2E-12	S	-
tbvl	SCR width modulation contribution	0	[0:inf)	4E-12	S	-
tef0	storage time in neutral emitter	0	[0:inf)	1E-12	S	-
gte	exponent factor for emitter transit time	1.0	(0:10]	1	-	-
thes	saturation time at high current densities	0	[0:inf)	3E-11	S	-
ahc	smoothing factor for current dependence	0.1	(0:10]	0.75	-	-
tr	storage time at inverse operation	0	[0:inf)	0	S	-
	Crit	tical Curre	nt			
rci0	low-field epi collector resistance under emitter	150	(0:inf)	50	Ω	1/M
vlim	voltage dividing ohmic and saturation region	0.5	(0:10]	0.7	V	-
vpt	punch-through voltage	inf	(0:100]	10	V	-
vces	saturation voltage	0.1	[0:1]	0.1	V	-
vdck	built-in BC voltage including voltage drop in B and C	0.0	[0:1]	0.0	V	-
delck	fitting factor for voltage dependence of critical current	2.0	(0:10]	2.0	-	-
aick	smoothing factor for ICK	1e-3	(0:10]	1e-3	-	-
_	Internal BC I	Depletion (	Capacitance			

# Table 3.0.0/1:

name	description	default	range	test	unit	factor
cjci0	internal zero-bias BC depletion capacitance	1E-20	(0:inf)	1.16E-15	F	M
vdci	BC built-in voltage	0.7	(0:10]	0.8	V	-
zci	BC exponent factor	0.333	(0:1]	0.333	-	-
vptci	punch-through voltage of BC junction	100	(0:100]	46	V	-
	External BC l	Depletion (	Capacitance		•	•
cjcx0	external zero-bias BC depletion capacitance	1E-20	[0:inf)	1E-20	F	M
vdcx	external BC built-in voltage	0.7	(0:10]	0.7	V	-
zcx	external BC exponent factor	0.333	(0:1]	0.333	-	-
vptcx	punch-through voltage	inf	(0:100]	100	V	-
fbc	factor for splitting either $C_{jc0}$ ( $C_{jx0}$ not specified) or $C_{jcx0}$ (if both $C_{jci0}$ and $C_{jcx0}$ specified)	1	[0:1]	0.1526	-	-
	Bas	e Resistano	ce			
rbi0	internal base resistance at zero-bias	0	[0:inf)	100	Ω	1/M
vr0e	reverse Early voltage (normalization volt)	2.5	(0:inf]	1.6	V	-
vr0c	forward Early voltage (nor- malization volt)	inf	(0:inf]	8	V	-
fgeo	geometry factor	0.656	[0:inf]	0.73	-	-
	Serie	s Resistan	ces		•	<u> </u>
rbx	external base series resistance	0	[0:inf)	8.8	Ω	-
rcx	external collector series resistance	0	[0:inf)	9.16	Ω	-
re	emitter series resistance	0	[0:inf)	12.5	Ω	-
	Substrate Transfer Currer	nt, Diode C	Current and C	Capacitance		

# Table 3.0.0/1:

name	description	default	range	test	unit	factor
itss	substrate transistor transfer saturation current	0	[0:1]	1E-17	A	-
msf	substrate transistor transfer current non-ideality factor	1.0	(0:10]	1.0	-	-
iscs	SC saturation current	0	[0:1]	1e-17	A	M
msc	SC non-ideality factor	1	(0:10]	1	-	_
cjs0	zero-bias SC depletion capacitance	1E-20	[0:inf)	1E-15	F	M
vds	SC built-in voltage	0.3	(0:10]	0.6	V	_
ZS	external SC exponent factor	0.3	(0:1]	0.447	-	_
vpts	SC punch-through voltage	inf	(0:100]	100	V	_
cbcpar	Parasii collector-base isolation (over-	tic Capacit	ance [0:inf)	1E-15	F	M
chenar	T	<u>-</u>		1E 15	F	М
_	lap) capacitance					
cbepar	emitter-base oxide capacitance	0	[0:inf)	2E-15	F	M
	BC Av	alanche Cu	irrent			
favl	prefactor	0	[0:inf)	1E-14	-	-
qavl	exponent factor	0	[0:inf)	1.19	-	-
	Fli	icker Noise	)			
kf	flicker noise coefficient	0	[0:inf)	0	-	M <sup>1-AF</sup>
af	af flicker noise exponent factor 2 (		(0:10]	2	-	-
Temperature Dependence						
vgb	bandgap-voltage	1.2	(0:10]	1.17	V	_
vge	effective emitter bandgap- voltage	- 1.17 (0:10] 1.1386		V	-	
vgc	effective collector bandgap- voltage	1.17	(0:10]	1.1143	V	-

# Table 3.0.0/1:

name	description	default	range	test	unit	factor
vgs	effective substrate bandgap- voltage	1.17	(0:10]	1.15	V	-
$\Delta v_{gBE}$	Bandgap difference between base and BE-junction. Used for temperature dependence of $V_{Er}$ and $I_{qf}$ .	0	-	0	-	-
flvg	coefficient K1 in T-dependent bandgap equation	1.0237 E-4		-1.0237E-4	V/K	-
f2vg	coefficient K2 in T-dependent bandgap equation	4.3215e -4		4.3215e-4	V/K	-
alt0	first-order TC of tf0	0	[-10:10]	0	1/K	-
kt0	second-order TC of tf0	0	[-10:10]	0	1/K <sup>2</sup>	-
zetavgbe	Temperature parameter for $V_{Er}$ .	1				
zetaver	Temperature parameter for <i>VEr</i> .	-1	-	-	-	-
zetact	exponent coefficient in trans- fer current temperature dependence	3	[-10:10]	3.5	-	-
zetabet	exponent coefficient in BE junction current temperature dependence	3.5	[-10:10]	4	-	-
zetaiqf	temperature coefficient for iqf	0	[-10:10]	0	-	-
zetaci	TC of epi-collector diffusivity	of epi-collector diffusivity 0 [-10:10] 1.6		-	-	
aliqfh	First order temperature coefficient for $I_{qfh}$ .	0	-			
kiqfh	Second order temperature coefficient for $I_{qfh}$ .	0	-			
alvs	relative TC of saturation drift velocity	0	[-10:10]	1E-3	1/K	-
alces	relative TC of vces	0	[-10:10]	4E-4	1/K	-

Table 3.0.0/1:

name	description	default	range	test	unit	factor
aldck	Relative TC of vces	0	-		1/K	-
zetarbi	TC of internal base resistance 0 [-10:10] 0		0.6	-	-	
zetarbx	TC of external base resistance	0	[-10:10]	0.2	-	-
zetarcx	TC of external collector resistance	0	[-10:10]	0.2	-	-
zetare	TC of emitter resistances	0	[-10:10]	0	-	-
alrth	First-order relative temperature coefficient of parameter Rth	0	[-10:10]	0	1/K	
zetarth	Exponent factor for temperature dependent thermal resistance	0	[-10:10]	0	-	-
alfav	Relative TC for FAVL	0	[-10:10]	0	1/K	-
alqav	Relative TC for QAVL	0	[-10:10]	0	1/k	-
	Vertic	al NQS Ef	fect		·	
flnqs	Flag for turning on and off of vertical NQS effects	0	0 or 1			
alit	Factor for additional delay time of transfer current	0.333	(0;1]			
alqf	Factor for additional delay time of minority charge	- I I I I I I I I I I I I I I I I I I I				
	Se	elf-Heating	5			
flsh	flag for turning on (1) or off (0) self-heating effect	0	0 or 1	1	-	-
rth	thermal resistance	0	[0:inf)	200	K/W	1/M
cth	thermal capacitance	0	[0:inf)	0.1	Ws/ K	M

Apart from the above list of the model parameters, there are few circuit simulator specific parameters as follows:

Table 3.0.0/2:

Circuit Simulator Specific Parameters					
name	description	default	test	unit	
tnom	temperature for which parameters are valid	27	27	°C	
dt	temperature change for particular transistor	0	0	K	
type	For transistor type NPN(+1) or PNP(-1)	+1			

• The reference temperature 27°C has been chosen to remain compatible with the usual simulator default. The desired temperature dependence of the bandgap (linear or nonlinear) can be adjusted by assigning proper values to f1vg and f2vg (K<sub>1</sub> and K<sub>2</sub>). Note that f1vg and f2vg are not necessarily HICUM-specific, but may be made general parameters in a simulator.

#### 4 Operating point information

In HICUM/L0v1.31, the operating point values are calculated directly inside the verilog-A code. A compiler flag "CALC\_OP" has been introduced, which enables the calculations inside the code when the flag is *turned-on* [17].

Below is the list of those quantities that should be provided in the circuit simulator output to the model users as "operating point information". The voltages in the expressions are defined as

$$V_{BEi} = V_{B'} - V_{E'}$$

$$V_{BCi} = V_{B'} - V_{C'}$$

Table 4.0.0/1:

Variable	Unit	Description	Definition	M factor
IB	A	Base terminal current	as calculated in the model	*M
IC	A	Collector terminal current	as calculated in the model	*M
IS	A	Substrate current	as calculated in the model	*M
IAVL	A	Avalanche current	as calculated in the model	*M
VBE	V	External BE voltage	as calculated in the model	-
VBC	V	External BC voltage	as calculated in the model	-
VCE	V	External CE voltage	as calculated in the model	-
VSC	V	External SC voltage	as calculated in the model	-
BETADC		Common emitter forward current gain	$\beta_{dc} = \frac{I_C}{I_B}$	-
GMi	A/V	Internal transconductance	$\left g_{mi} = \left. \frac{\partial I_T}{\partial V_{BEi}} \right _{V_{CEi}} = \left. \frac{\partial I_T}{\partial V_{BEi}} \right _{V_{BCi}} + \left. \frac{\partial I_T}{\partial V_{BCi}} \right _{V_{BEi}}$	*M
RPIi	Ω	Internal input resistance	$\frac{1}{r_{\pi i}} = \left. \frac{\partial I_{BEi}}{\partial V_{BEi}} \right _{V_{BCi}}$	/M

Table 4.0.0/1:

Variable	Unit	Description	Definition	M factor
RMUi	Ω	Internal feedback resistance	$\frac{1}{r_{\mu i}} = \frac{\partial I_{BCi}}{\partial V_{BCi}} - \frac{\partial I_{AVL}}{\partial V_{BCi}}\Big _{V_{BEi}}$	/M
ROi	Ω	Internal Output resistance	$\left  \frac{1}{r_{oi}} = -\frac{\partial I_T}{\partial V_{BCi}} \right _{V_{BEi}} + \frac{\partial I_{AVL}}{\partial V_{BCi}} \right _{V_{BEi}}$	/M
CPIi	F	Total BE capacitance	$C_{\pi i} = C_{jE} + C_{dE} + C_{BEpar}$	*M
CMUi	F	Total internal BC capacitance	$C_{\mu i} = C_{jCi} + C_{dC}$	*M
CBCX	F	Total external BC capacitance	$C_{BCx} = C_{jCx} + C_{BCpar}$	*M
CCS	F	CS junction capacitance	$C_{CS} = C_{jS}$	*M
RBi	Ω	Internal base resistance	$r_{Bi}$	/M
RB	Ω	Total base resistance	$r_B = r_{Bi} + r_{Bx}$	/M
RCX	Ω	External (saturated) collector series resistance	Model parameter $R_{CX}$	/M
RE	Ω	Emitter series resistance	Model parameter $R_E$	/M
ВЕТААС		Small signal current gain	$\beta_{ac} = g_{mi} \cdot r_{\pi i}$	-
TF	S	Total forward transit time	as calculated in the model	-
FT	Hz	Transit frequency (Note this is an approximation)	$f_{T} = \frac{g_{mi}}{2\pi \cdot (C_{BE} + C_{BC} + r \cdot C_{BC} \cdot g_{mi})},$ $C_{BE} = C_{\pi i},$ $C_{BC} = C_{\mu i} + C_{BCx},$ $r = R_{Cx} + R_E + \frac{R_B + R_E}{\beta_{ac}}$	-

Note: The variables GMi, RPIi, RMUi, ROi, CPIi, CMUi represent the accurate designation compared to the corresponding variables GM, RPI, RMU, RO, CPI, CMU of the SGP model.

HICUM/L0 References

#### **5** References

[1] M. Schröter and A. Chakravorty, "Compact hierarchical modeling of bipolar transistors with HICUM", World Scientific, Singapore, ISBN 978-981-4273-21-3, 2010.

- [2] J. Paaschens and W. Kloosterman, "The MEXTRAM Bipolar Transistor Model, Level 504", Nat. Lab. Unclassified Report NL-UR2000/811, Sept. 2001.
- [3] C. McAndrew et al., "VBIC95, the vertical bipolar intercompany model", IEEE J. Solid-State Circuits, Vol. 31, pp. 1476-1483, 1996.
- [4] M. Schroter, S. Lehmann, S. Fregonese, T. Zimmer, "A computationally efficient physics-based compact bipolar transistor model for circuit design Part I: model formulation", IEEE Transaction on Electron Devices, Vol. 53, No. 2, pp. 279-286, 2006
- [5] S. Fregonese et al., "A computationally efficient physics-based compact bipolar transistor model for circuit design Part II: Experimental results". IEEE Transaction on Electron Devices, Vol. 53, No. 2, pp. 287-295, 2006
- [6] M. Schröter, H.-M. Rein, W. Rabe, R. Reimann, H.-J. Wassener and A. Koldehoff, "Physics-and process-based bipolar transistor modeling for integrated circuit design", IEEE Journal of Solid-State Circuits, Vol. 34, pp. 1136-1149, 1999.
- [7] M. Schröter, Z. Yan, T.-Y Lee and W. Shi, "A compact tunneling current and collector breakdown model", Proc. IEEE Bipolar Circuits and Technology Meeting, Minneapolis, pp. 203-206, 1998.
- [8] M. Schroter and T.-Y. Lee, "A physics-based minority charge and transit time model for bipolar transistors", IEEE Trans. Electron Dev., vol. 46, pp. 288-300, 1999.
- [9] M. Schroter and D.J. Walkey, "Physical modeling of lateral scaling in bipolar transistors", IEEE J. Solid-State Circuits, Vol. 31, pp. 1484-1491, 1996 and Vol. 33, p. 171, 1998.
- [10] M. Schroter, M. Friedrich, and H.-M. Rein, "A generalized Integral Charge-Control Relation and its application to compact models for silicon based HBT's", IEEE Trans. Electron Dev., Vol. 40, pp. 2036-2046, 1993.
- [11] C.Thiele (Infineon), "Further developments of the HICUM/L0 model"; 8th HICUM Workshop, Böblingen, Germany, May, 2008.
- [12] C. Thiele, J.Berkner, W.Klein, "Improvement of the Transfer Current Modeling in HICUM/LO", BCTM 2007, pp. 62-65.
- [13] C. Thiele, W.Klein, "A new explicit expression for the normalized hole charge improves the accuracy of HICUM/L0", pp. 77-80, BCTM 2008.
- [14] A. Pawlak, M. Schröter, J. Krause, "A HICUM extension for medium current densities", 9th HICUM Workshop, Würzburg, Germany, October, 2009
- [15] H.-M. Rein and M. Schröter, "A compact physical large-signal model for high-speed bipolar transistors at high current densities Part II: Two-dimensional model and experimental results", IEEE Trans. Electron Dev., Vol. 34, pp. 1752-1761, 1987.
- [16] M. Schroter, "Simulation and modeling of the low-frequency base resistance of bipolar transistors in dependence on current and geometry", IEEE Trans. Electron Dev., Vol. 38, pp. 538-544, 1991.
- [17] Internal report, "Vertical NQS-modeling and output of operating point values", CEDIC, 2012.
- [18] S. Lin and C. Salama, "A V<sub>BE</sub>(T) model with application to bandgap reference design", IEEE Journal of Solid-State Circuits, Vol. 20, pp. 1283-1285, 1985.
- [19] D. Celi, private communications, 2004.

HICUM/L0 References

- [20] www.tiburon-da.com
- [21] L. Lemaitre, C. McAndrew and S. Hamm, "ADMS Automatic device model synthesizer", Proc. Custom Integrated Circuits Conf., pp. 27-30, 2002.
- [22] A. Pawlak, M. Schröter, A. Mukherjee, S. Lehmann, S. Shou, D. Celi, "Automated Model Complexity Reduction using the HICUM Hierarchy", IEEE SCD, 4 pages, 2011.

[23] http://www.iee.et.tu-dresden.de/iee/eb/hic\_new/hic\_intro.html

# 6 Appendix

#### **6.1 Parameter Extraction**

HICUM/L0 has been derived from the more sophisticated and accurate HICUM/L2 model, hence the parameter extraction can be done in two different ways: (i) calculation of HICUM/L0 parameters directly from HICUM/L2 parameters and characteristics, or (ii) extraction directly from measured characteristics of a given transistor. Below, these options are briefly discussed.

#### 6.1.1 Parameter determination of HICUM/L0 from HICUM/L2

Many parameters can be calculated directly from the HICUM/L2 parameter set, e.g., CS, BE, BC diode current and depletion charge, series resistances with most of the parameters for the internal base resistance, self-heating, temperature dependence (many of the coefficients), parasitic substrate transistor, transit time (most parameters), avalanche current [1, 15]. Also, useful initial values for the remaining parameters of the transfer current and transit time can be generated from HICUM/L2. An fully automated "L2-to-L0" converter has been developed [22], which can be used to generate L0 model parameter sets directly from those of L2 for given discrete transistor geometries.

#### 6.1.2 Parameter extraction from experimental data

The simplicity of HICUM/L0 allows extractions on single (discrete) transistors. Table 6.1.2/1 contains the possible flow of a step-by-step extraction procedure is described here. Due to the strong self-heating in advanced process technologies it is recommended to determine the temperature dependent parameters early in the procedure to enable possible corrections during the extraction of the other parameters.

Table 6.1.2/1:

Step	EC Element	Parameters
1	Total BE, BC, and CS depletion capacitances	$\begin{array}{c} C_{jE0}, V_{DE}, z_E \ C_{jCi0}, V_{DCi}, z_{Ci}, \\ V_{PTCi} \ , C_{jCx0}, V_{DCx}, z_{Cx}, V_{PTCx} \ , \\ C_{jS0}, V_{DS}, z_S \end{array}$
2	Base current components related to BE and BC junction CS substrate junction current	$I_{BES}$ , $m_{BE}$ , $I_{RES}$ , $m_{RE}$ , $I_{BCS}$ , $m_{BC}$ , $I_{SCS}$ , $m_{SC}$

Table 6.1.2/1:

Step	EC Element	Parameters
3	Temperature coefficients self-heating	TCs of R <sub>TH</sub> , C <sub>TH</sub>
4	Series resistances	$r_{Cx}, r_E, r_{Bx}, r_{Bi0}, V_{r0E}, V_{r0C}, f_{geo}$
5	Transfer current at low and medium injection	$\begin{aligned} &\mathbf{I_{S}, m_{Cf}, m_{Cr}, V_{Ef}, V_{Er}, V_{DEdc},} \\ &\mathbf{z_{Edc}, a_{jEdc}, C_{jCdc}, V_{DCdc}, V_{PTdc}} \end{aligned}$
6	BC Avalanche current	e <sub>AVL</sub> , k <sub>AVL</sub>
7	Transit time at low injection	$ au_0,  au_{\mathrm{Bvl}}, \Delta  au_{0\mathrm{h}}, a_{\mathrm{jE}}$
8	Critical current	$r_{Ci0}, V_{CEs}, V_{PT}, V_{lim}$
9	Transit time at high injection	$ au_{\mathrm{Ef0}},  \mathbf{g}_{\mathrm{\tau E}},  \mathbf{\tau}_{\mathrm{hcs}},  \mathbf{a}_{\mathrm{hc}}$
10	Transfer current at high injection	I <sub>Qf</sub> , I <sub>Qr</sub> , I <sub>Qfh</sub> , t <sub>fh</sub> , a <sub>hq</sub>
11	Remaining parameters and fine tuning	K <sub>F</sub> , A <sub>F</sub>

#### 6.2 Solution of transfer current equation

The general normalized form for of a third-order equation can be written as

$$x^3 + ax^2 + bx + c = 0 , (6.2-1)$$

with the coefficients

$$a = -\left(1 + \frac{q_{jE}}{V_{Er}} + \frac{q_{jC}}{V_{Ef}}\right), b = -\left(\frac{i_{Tfi}}{I_{CKf}} + \frac{i_{Tri}}{I_{CKr}} + w^2 \frac{I_{Tfi}}{I_{Qfh}}\right) \text{ and } c = -\frac{I_{Tfi}^2 t_{fh}}{I_{CK} I_{Qfh}}.$$
 (6.2-2)

The third-order equation can be transformed to a *depressed-cubic* equation using the transformation  $x = z - \frac{a}{3}$ , which allows to eliminate the second-order term. The equation now reads,

$$z^3 + pz + q = 0 , (6.2-3)$$

The values of p and q are given by;

$$p = b - \frac{a^2}{3}$$
 and  $q = \frac{2a^3}{27} - \frac{ab}{3} + c$ . (6.2-4)

The number of real solutions depends on the value of the determinant

$$D = \left(\frac{q}{2}\right)^2 + \left(\frac{p}{3}\right)^3 . \tag{6.2-5}$$

For low injection in either forward and reverse case, the values of both, b and c tend towards zero, leading to D = 0 and thus

$$z = \frac{3q}{p} = -\frac{2a^3}{9} \frac{3}{a^2} = -\frac{2}{3}a \ . \tag{6.2-6}$$

This gives the following solution:

$$x = -\frac{2}{3}a - \frac{1}{3}a = -a = 1 + \frac{q_{jE}}{V_{Er}} + \frac{q_{jC}}{V_{Ef}}.$$
 (6.2-7)

For reverse operation, c tends towards zero. This is also the case if tfh is set to zero, resulting in

$$D = \frac{4b^3 - b^2 a^2}{108},\tag{6.2-8}$$

which is negative in all cases. In this case, complex solutions are possible. For evaluating the solution, only the angles for the third roots need to be calculated. The value of

$$\delta = \operatorname{acos}\left(-\frac{q}{2}\sqrt{-\frac{27}{p^3}}\right), \tag{6.2-9}$$

is used for reference. If a >> b, the argument is one. However, with increasing b, the argument tends toward zero. Therefore, the resulting angle will be in all cases between  $\theta^{\circ}$  and  $\theta^{\circ}$ . The three solutions are calculated as

$$z_{1} = -\sqrt{-\frac{4}{3}p\cos\left(\frac{1}{3}\delta - \frac{\pi}{3}\right)}, z_{2} = -\sqrt{-\frac{4}{3}p\cos\left(\frac{1}{3}\delta\right)}, z_{3} = -\sqrt{-\frac{4}{3}p\cos\left(\frac{1}{3}\delta + \frac{\pi}{3}\right)}$$
 (6.2-10)

Though three different values of z are possible, the maximum value of  $z_1$  and  $z_3$  will be zero, which finally leads to a maximum of  $x_{1/3} = -\frac{a}{3}$ . Hence both solutions are not meaningful. Only  $z_2$  and its corresponding value for  $x_2$  (i.e.  $q_{pt}$ ) have been considered since they lead to a physically meaningful result and therefore correct values.

For the remaining case, when D is positive, only one physically correct solution exists and both

$$u = \sqrt[3]{-\frac{q}{2} + \sqrt{D}}$$
 and  $v = \sqrt[3]{(-\frac{q}{2}) - \sqrt{D}}$  (6.2-11)

are real numbers. The only real solution then reads

$$z_1 = u + v$$
 with the corresponding  $x_1 = z - \frac{a}{3}$ . (6.2-12)